Upgrading of bio-oil from biomass pyrolysis over Cu-modified β-zeolite catalyst with high selectivity and stability

Wahyu Bambang Widayatno[a], Guoqing Guan[a,b,*], Jenny Rizkiana[a], Jingxuan Yang[b,c], Xiaogang Hao[c], Atsushi Tsutsumi[d], Abuliti Abudula[a,b,*]

[a] Graduate School of Science and Technology, Hirosaki University, 1-Bunkyocho, Hirosaki 036-8560, Japan
[b] North Japan Research Institute for Sustainable Energy (NJRISE), Hirosaki University, 2-1-3, Matsubara, Aomori 030-0813, Japan
[c] School of Chemistry and Chemical Engineering, Taiyuan University of Technology, Taiyuan 030024, China
[d] Collaborative Research Center for Energy Engineering, Institute of Industrial Science, The University of Tokyo, 4-6-1 Komaba, Meguro-ku, Tokyo 153-8505, Japan

ARTICLE INFO

ABSTRACT

Upgrading of bio-oil from biomass pyrolysis over Cu-modified β-zeolite catalyst in a down-draft fixed-bed reactor, in which the pyrolysis and upgrading processes are integrated, is investigated in details. It is found that high silica β-zeolite has high selectivity to the hydrocarbon during the upgrading process. When it is modified by a small amount of Cu, the selectivity can be obviously promoted. Especially, when 0.50 wt% of Cu is loaded on it, almost only hydrocarbons can be detected in the light oil of upgraded bio-oil and its activity can be remained for several reuses even without regeneration treatment. However, if more Cu is loaded, the selectivity decreases to some extent. Interestingly, low Cu loading on β-zeolite results in the increase of surface area as well as the formation of more micropores. The surface area reaches the maximum in the case of 0.50 wt% of Cu doping. Based on XRD analysis, when the loading amount is over 1.00 wt%, Cu species aggregate on the surface of zeolite, resulting the blockage of zeolite pores and the decrease of surface area. Doping of Cu decreases the coke deposit on spent catalyst but overloading of Cu results in the increase of coking and the decrease of activity and selectivity. These results indicate that the synergetic effect between the doped metal sites and the protonic sites on the zeolite structure should be benefit for the promising catalytic performance and thus, a proper loading amount is very important for this kind of catalyst.

© 2016 Elsevier B.V. All rights reserved.

1. Introduction

Recently, biomass conversion to high-quality bio-oil has become an important issue due to its potential to solve fossil fuels shortage and environmental problems [1–7]. Fast pyrolysis of biomass is a simple way to obtain bio-oil with high yield. Unfortunately, the obtained raw bio-oil is generally corrosive, unstable and immiscible with petroleum fuels; especially, it has low heating value due to a large amount of oxygenated compounds included [6,8–10]. Therefore, the raw bio-oil needs to be upgraded by removing oxygenated compounds to satisfy the requirements of boiler fuel or the additive for the existing fossil fuel. To achieve this objective,

two major approaches, i.e. catalytic hydroprocessing over metal-based catalysts [11,12] and catalytic cracking over porous materials [13,14], are always applied. Catalytic hydroprocessing involves catalytic hydrocracking, hydrodeoxygenation and hydrotreatment, by which the high grade bio-oil with low oxygen amount and high H/C ratio can be obtained. However, it requires considerable amount of hydrogen which is too expensive for a practical process. As an alternative, catalytic cracking over catalysts with porous structure receives more attention in bio-oil upgrading study. This method mimics the process of fluid catalytic cracking of crude oil by using zeolites. To date, various zeolites have been tried to upgrade bio-oils [15–19]. Lee et al. found that HZSM-5 zeolite can selectively convert oxygenates species in the bio-oil to aromatics compounds due to its small pore opening and strong acidity. However, they indicated that HZSM-5 zeolite cannot completely decompose large oxygenate species, and suggested that zeolites with larger pore such as Hβ and HY are more benefit for this purpose [18]. Ramasamy et al. also found that HZSM-5 can be only applied for converting those

* Corresponding authors at: North Japan Research Institute for Sustainable Energy, Hirosaki University, 2-1-3 Matsubara, Aomori 030-0813, Japan. Fax: +81 17 735 5411.
E-mail addresses: guan@hirosaki-u.ac.jp (G. Guan), abuliti@hirosaki-u.ac.jp (A. Abudula).

small oxygenates in the bio-oil. Moreover, they proposed different mechanisms on the competitive adsorption of oxygenates with different functional group on the active sites [17]. On the other hand, it is found that coke formation easily occurs on HY zeolite due to its large pore opening, [20]. In our previous study [15], Hβ zeolite with moderate pore opening is found to have high selectivity to hydrocarbons with low coke formation when comparing with other zeolites.

To enhance the catalytic activity of zeolite for various reactions, metal is usually loaded on zeolite [21–26]. However, to the best of our knowledge, only a few studies reported Cu-modified zeolites for the upgrading bio-oil. Du et al. found that Cu-modified HZSM-5 can increase hydrocarbons yield significantly [24]. The similar result is also presented by Veses et al [21]. However, nobody reported the stability and reusability of the catalysts in the case without regeneration, which is important in a practical process for avoiding activity degradation by thermal regeneration [27,28].

Based on our previous study [15], in this study, Cu-modified β-zeolite with various loading amounts were synthesized and applied for upgrading bio-oil in a down-draft fixed-bed reactor, in which the pyrolysis and upgrading processes are integrated. The optimum Cu loading amount was obtained and its reusability in the case without regeneration was investigated. To understand the catalytic mechanism of converting oxygenates species in the bio-oil on the Cu-modified β-zeolite, the relationship of crystal structure, pore properties, and acid site distribution of the catalysts with the Cu loading amount was elaborated. The oxidation of coke on the spent catalyst was analyzed to understand the relationship of Cu loading amount with the formed coke species. It is expected that the obtained catalyst can be applied to upgrade bio-oil effectively.

2. Materials and methods

2.1. Catalyst preparation and characterization

High silica β-zeolite (HSZ-960, Si/Al = 100) in its protonic form (H^+ cation) was purchased from TOSOH Corporation and used without further treatment. Copper was loaded on it using wet impregnation method. Firstly, the parent zeolite powder was dispersed in copper nitrate solution. After stirring at room temperature for 2 h, the solution was continuously stirred on hot plate until the mixture was dried. Then, the dried mixture were calcined in air at 650 °C for 3 h. As a result, 0.25, 0.50, 1.00 and 3.00 wt% of Cu loaded β-zeolite catalysts were prepared. For catalytic comparison, the as-received β-zeolite was also calcined at the same condition and was denoted as calcined β-zeolite.

Surface area and pore property of the catalyst were examined by N_2-adsorption measurement equipment (NOVA 4200e, Quantachrome Instruments, USA). The calcined catalysts were vacuum-degassed at 250 °C for 2 h before the measurement. The total surface area was determined using Brunauer-Emmet-Teller (BET) method while the surface area and volume of micropores was calculated using t-plot method from the isotherm profile. The obtained results are shown in Table 1.

Crystalline structure of the calcined catalysts were analyzed using X-ray Diffraction (XRD) (Smartlab, Rigaku, Japan). Distribution of acid sites on the calcined catalyst was determined by conducting the NH_3-desorption (NH_3-TPD) measurement (Belcat, Japan). Briefly, 0.1 g catalyst was loaded in the measurement cell and pretreated at 500 °C under 50 cm^3/min He flow to release the adsorbed moisture from the catalyst pores. After 1 h pretreatment at that temperature, the catalyst was cooled down to 120 °C and stabilized for 10 min. Thereafter, 50 cm^3/min NH_3 stream was flowed into the measurement cell for 1 h. Before conducting the desorption step, the catalyst was flushed by 50 cm^3/min He stream

Table 1
Summary of N_2 adsorption test.

Cu loading (wt%)	0.00	0.25	0.50	1.00	3.00
S_{BET}[a] (m^2/g)	410	477	520	518	499
S_{Micro}[b] (m^2/g)	385	432	475	473	455
S_{Meso}[c] (m^2/g)	25	45	45	45	44
V_{Total}[a] (cm^3/g)	0.25	0.31	0.32	0.31	0.30
V_{Micro}[b] (cm^3/g)	0.19	0.23	0.24	0.24	0.23
V_{Meso}[c] (cm^3/g)	0.06	0.08	0.08	0.07	0.07
Avg. pore size[d] (nm)	2.47	2.47	2.43	2.42	2.41

[a] BET method.
[b] t-Plot method.
[c] By difference.
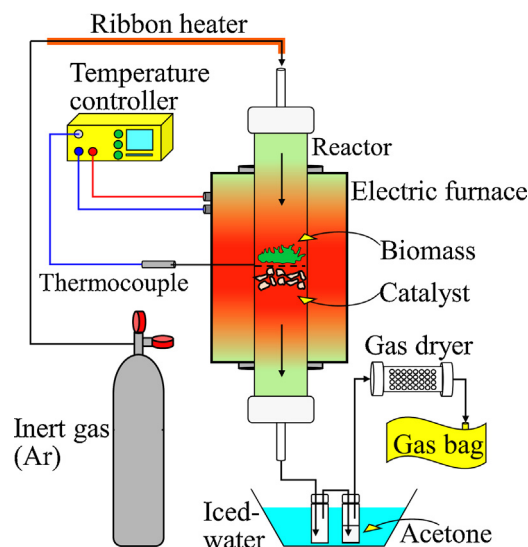[d] Average of micropore and mesopore.

Fig. 1. Schematic of experimental setup for catalytic upgrading of bio-oil.

for 5 h to remove the physically-adsorbed NH_3 and ensure only the chemically-adsorbed NH_3 was remained on the catalyst surface. After stabilization at 120 °C for 10 min, the NH_3 desorption was carried out until 900 °C with a heating rate of 10 °C/min. The desorbed NH_3 was flushed by 50 cm^3/min He to Thermal Conductivity Detector (TCD). The amount of the desorbed NH_3 was calculated by converting the measured TCD voltage using the calibration data in the machine and presented as a function of temperature. Meanwhile, the reduction temperature position of the Cu-modified β-zeolite was examined by conducting H_2-Temperature Programmed Reduction (H_2-TPR) using the same machine and pretreatment method as that for NH_3-TPD. After cooled to room temperature, H_2-TPR was carried out by flowing H_2 from room temperature to 700 °C.

2.2. Catalytic activity and selectivity

Stem part of Japanese knotweed (*Fallopia Japonica*) was used as biomass feedstock in this study. The details of its properties have been described elsewhere [29]. Pyrolysis of biomass and catalytic upgrading of the generated bio-oil over the catalyst were conducted simultaneously in a down-draft fixed bed reactor which is shown in Fig. 1. Briefly, 2 g of catalyst bed was placed under 0.6 g biomass feedstock in the stainless steel reactor at first and then, the reactor was heated to 600 °C under argon flow with a heating rate of 80 °C/min, and held at that temperature for 30 min. To investigate the reusability and deactivation resistance of the catalyst, it was used for four consecutive tests without regeneration, which are

denoted as fresh, r-1, r-2, and r-3, respectively. All experiments were repeated for at least two times.

Liquid products were entrapped in two serial ice-cold traps, where acetone was used in the second cold trap to ensure the entrapment of all liquid products. The obtained liquid products were then fractionated to the heavy fraction (boiling point >300 °C), which cannot be detected by GC–MS, and the light fraction of bio-oil (boiling point <300 °C; called "light oil" here). Chemical compositions of the light oil were evaluated by Gas Chromatography and Mass Spectroscopy method (GC-2010 Plus and GC/MS-QP2010 Ultra, Shimadzu Japan) with Ultra ALLOY+ −5 capillary column. The built-in NIST database was used as a reference to determine the chemicals contained in the light bio-oil. The yields of components in the light oil were calculated based on the initial dry ash-free biomass. Water content in the bio-oil was detected using Karl-Fischer titration method (MKS-500, KEM Japan). Gaseous products were collected in a gas bag after flowed through a gas dryer chamber and analyzed by gas chromatography (GC 7890A, Agilent Technologies USA).

Solid products and deposited coke for each experiment were estimated using analytical balance. Herein, the deposited coke was estimated by comparing the weight of catalyst before and immediately after the reaction.

2.3. Analysis of coke deposit on spent catalysts

The total coke deposit amount after four consecutive test was quantified using Thermogravimetry Analysis (DTG-60H, Shimadzu, Japan) and presented as the percentage of residual mass of spent catalysts. Briefly, about 10 mg of the spent catalyst was loaded on alumina crucible and preheated at 120 °C for 30 min to remove the contribution of moisture at first and then, the sample was heated to 800 °C with a heating rate of 5 °C/min. The carbon species on the spent catalyst was analyzed using Temperature Programmed Oxidation (TPO) method. About 0.1 g of the spent catalyst was loaded in the measurement cell and pretreated in argon atmosphere at 120 °C for 2 h and then, the sample was cooled to 40 °C. Thereafter, the oxidation of spent catalyst was carried out by flowing the mixture of 1% O_2 v/v in argon with a heating rate of 5 °C/min until 900 °C. It should be noted here that the pre-treatment was carried out at much lower temperature than that of NH_3-TPD pre-treatment temperature, to minimize the possibility of releasing the weakly-bonded coke from the catalyst surface.

3. Results and discussion

3.1. Properties of Cu-modified β-zeolite catalysts

In general, when metal is loaded on porous support, the surface area will decrease due to the pore blockage and metal sintering during the calcination step, as mentioned in the literatures [11,21,23]. However, in the present study, as shown in Table 1, Cu loading results in the increase of the total surface area. One can see that such an increase is contributed mainly by the increase of micropore surface area. Here, in the case of low Cu loading amount, the small Cu species might enter the zeolite channel and possibly generate new surface area within the channel by increasing the surface roughness. On the other hand, Cu species loaded on the external surface of zeolite could generate new mesopore surface area. As shown in Table 1, the maximum surface area appears at 0.50 wt% of Cu loading amount. However, with the more increase in Cu loading amount, either the micropore or mesopore surface area shows a decreasing trend, which should be resulted from the pore blocking and/or the sintering of Cu species. The pore blocking was also confirmed with the decreasing trend of pore volume and average pore
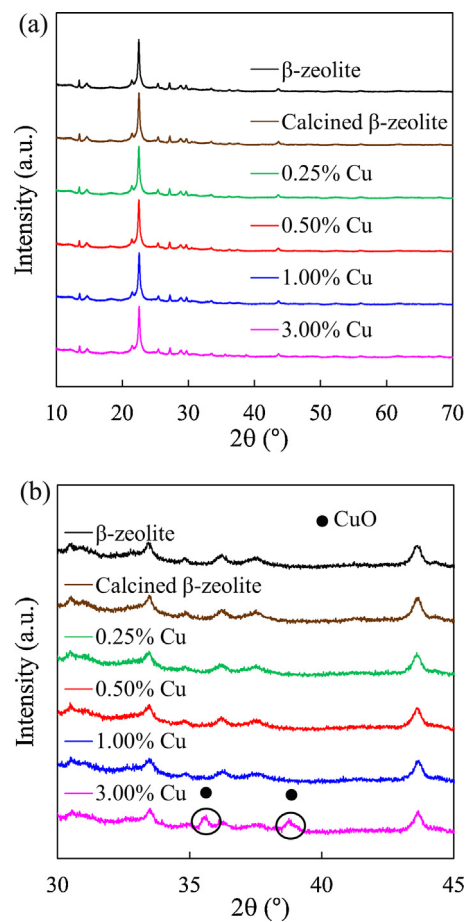

Fig. 2. XRD patterns of Cu-modified β-zeolites after calcination.

size at higher Cu loading amount. It should also be noted from Fig. S1 that the isotherms of the calcined β-zeolite and its Cu-modified counter parts reveal the hysteresis and have some difference with that of the microporous material (Type I isotherm), suggesting the existence of some mesopores Hence, the obtained average pore size involves both of the micropore and mesopore.

Fig. 2 shows XRD spectra of Cu-modified β-zeolites with different loading amounts. One can see from Fig. 2a that the XRD patterns of the as-received β-zeolite, the calcined counterpart and the Cu-modified β-zeolites with low Cu loading amount are almost the same, suggesting that the structure of β-zeolite is still preserved during calcination at 650 °C. In a more detail observation from Fig. 2b, the peaks related to CuO species can be only observed clearly in the cases of high loading amounts, i.e., 3 wt% of Cu loading amount. In contrast, no peaks corresponding to Cu species can be observed in the cases of low Cu loadings (<1.00 wt% of Cu loading amount), suggesting the good dispersion of Cu species in zeolite, which is also in agreement with the results of N_2 adsorption test. The low Cu loading ensures the physical separation of Cu species and avoids the agglomeration of small particles to larger crystallites during the calcination [30]. Furthermore, as mentioned above, the small Cu species could enter into the zeolite channel and replace the H^+ cation on the zeolite inner surface so that the inner surface roughness increases to some extent.

Fig. 3 presents NH_3-TPD profiles of Cu-modified β-zeolites with different loading amounts, which are also summarized in Table 2. One can see that the similar TPD profiles are shown for those samples with a Cu loading amount less than 1.00 wt%. Using the calcined β-zeolite as a basis, the acid sites of the catalysts can be divided into low temperature (LT, ≤500 °C) and high temperature
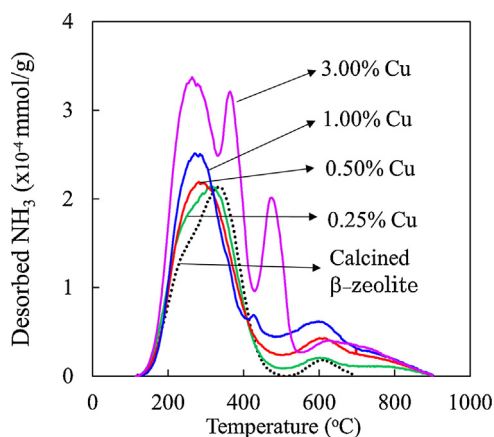
Fig. 3. NH$_3$-TPD profiles of Cu-modified β-zeolites.

Table 2
Acid sites distributions in Cu-modified β-zeolites.

Cu loading (wt%)	Low temp. sites (mmol/g)	High temp. sites (mmol/g)	Total acid sites (mmol/g)
0.00	0.219	0.009	0.228
0.25	0.237	0.028	0.265
0.50	0.258	0.057	0.315
1.00	0.252	0.090	0.342
3.00	0.413	0.142	0.555

(HT, >500 °C) acid sites. It should be noted that the low temperature peak shifts to low temperature direction with the increase of Cu loading amount for these samples. Pereda-Ayo et al. reported that isolated Cu species are likely to be dominant at low Cu loading [31]. Thus, such a shifting of low temperature peak should be attributed to the replacement of H$^+$ cations with Cu^{2+} cations which increase the low temperature acid sites amount. When Cu loading amount is increased to 1.00 wt%, a small peak at about 431 °C appears and the low temperature peak shifts more significantly to lower temperature. The obvious change is observed for 3.00 wt% Cu loading amount, which is also confirmed by XRD analyses. Veses et al. reported that various Cu species such as isolated Cu^{2+} ions, Cu^{2+}O$^-$ and Cu^{2+}O^{2-}Cu^{2+} compounds, and CuO clusters could appear at high Cu loading amount [21]. Herein, considering the decrease of surface area, the obvious CuO peaks appeared on XRD patterns, and the evolved peaks and significant increase of TPD peaks, it is highly possible that the occurrence of large Cu species clusters could generate excess acid sites i.e., metal/metal-oxide sites. In general, the increase of active site amount favors the catalytic reaction. However, it might also contain some Lewis acid sites which could promote the coking and result in deactivation due to the dehydration reaction to produce coke precursor [32,33]. Thus, considering the differences of TPD profiles and the significant increase of low temperature (LT) acid site amount, the Cu species clusters are highly possible to generate different types of acid sites, which might affect either the catalytic performance or the deactivation resistance.

The existence of agglomerated CuO species at higher Cu loading was also confirmed from the H$_2$-TPR profiles of the calcined fresh catalysts in Fig. S2. Here, since no more peaks are detected at higher temperature, the TPR profile is only presented until 450 °C. One can see that no peak appears at low Cu loading (0.25 and 0.50 wt%), suggesting that no reducible species exists in these catalysts. On the contrary, small peak can be observed at about 185 °C for 1.00 wt% Cu loading, such a peak becomes more intense and shifts to higher temperature (about 208 °C) for 3.00 wt% Cu loading, which suggests the existence of reducible CuO species for 1.00
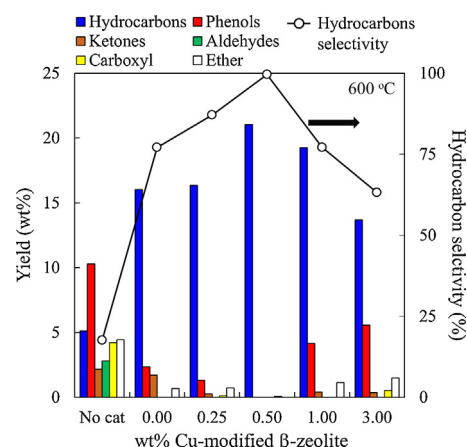

Fig. 4. The yields of various components and the hydrocarbon selectivity in the light oil of bio-oil in the presence and absence of catalysts.

and 3.00 wt% Cu loadings. Here, the peak intensity difference of 1.00 and 3.00 wt% Cu-modified β-zeolite can be attributed to the different amounts of reducible CuO species. Moreover, the peak related to the start and the end of the reduction should be resulted from the interaction between CuO species and β-zeolite support. The lower reduction starting temperature of 3.00 wt% Cu-modified β-zeolite can be attributed to the higher amount of larger CuO particles which have lower interaction with β-zeolite support when compared with that of 1.00 wt% Cu-modified one. This is in agreement with the XRD observation which proves the existence of agglomerated CuO species.

3.2. Catalytic performance of Cu-modified β-zeolite for bio-oil upgrading

Fig. 4 shows the yields of various components and the hydrocarbon selectivity in the light oil of bio-oil in the presence and absence of catalysts. The complete chemicals identification of the light oil can be found in Table S1 and Fig. S3 of Supplementary data. One can see that more hydrocarbons are detected in the light oil when the calcined β-zeolite itself is used, indicating that it has good catalytic selectivity for the conversion of the oxygenated compounds in raw bio-oil to hydrocarbons. When it is modified by a small amount of Cu, the selectivity can be obviously promoted. Especially, when 0.50 wt% of Cu is loaded on it, almost only hydrocarbons can be detected in the light oil, indicating that most oxygenated components in the bio-oil are converted to hydrocarbons. As indicated above, 0.50 wt% Cu-modified β-zeolite has the highest surface area and more low temperature acid sites, which are benefit for the deoxygenation reaction. Herein, it should be also noted that the low amount of Cu loading obviously results in a significant decarbonylation of those compositions in raw bio-oil, which is indicated by the significant decrease of ketones and aldehydes compounds [21]. However, more Cu loading results in the decrease of hydrocarbons yield even though the acid site amount increases considerably from TPD analysis. For 1.00 wt% of Cu loading amount, even though the hydrocarbons yield in the light oil is still high, the selectivity decreases and its catalytic activity is almost similar to the calcined β-zeolite. The decrease of hydrocarbons in the light oil is accompanied by the increase of phenolic compounds and ketones, which become more pronounced for 3.00 wt% of Cu loading amount. As shown above, considering the change of physical properties and contrast difference of TPD profile for the high Cu-loading cases, the change of catalytic activity and the selectivity for them are reasonable. For high Cu loading (i.e. more than 1.00 wt%), the Cu species might be not dispersed well on the zeolite and some large
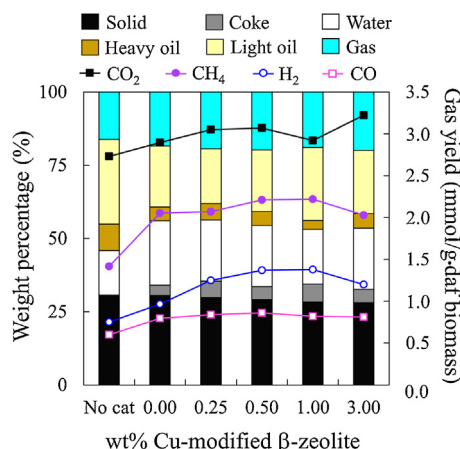
Fig. 5. Mass balance of the final products in the presence and absence of catalysts.

Cu species cluster will be formed on the surface of zeolite, which will significantly inhibit the contact between reactant and zeolite surface.

Fig. 5 presents the mass balance of the products in the presence and absence of catalysts. Herein, the proportion of each pyrolysis products is presented in percentage with respect to the initial amount of biomass (dry ash free base). One can see that the yields of CO slightly increase to some extent for Cu-modified β-zeolites, indicating that Cu-modified β-zeolite can further promote decarbonylation reactions. It should be noted that less heavy oil is remained when using Cu-modified β-zeolite, suggesting that they have better cracking activity. Especially, considering the higher gaseous products and hydrocarbons selectivity, 0.5 wt% Cu-modified β-zeolite possesses better performance for deoxygenation of bio-oil. One can see that less heavy oil remains in the upgraded bio-oil when using 1.00 wt% Cu-modified β-zeolite, however, as shown in Fig. 4, its selectivity is lower than 0.5 wt% Cu-modified. It is possible that some of the cracked products could not be further deoxygenized but deposited on the catalyst surface. For 3.00 wt% Cu-modified β-zeolite, more CO_2 and less CH_4 and H_2 are obtained. The increased CO_2 could be generated from the reduction of CuO by the reductive pyrolysis gas because more agglomerated CuO exists on the outer surface of β-zeolite at high Cu loading, as proved from XRD and H_2-TPR observations. In this case, more Cu species could appear on the catalyst, which will be also benefit for the cracking of hydrocarbons and result in more coke deposit on the catalyst surface. Similar finding about this has been reported before [23]. In addition, the water-gas shift reaction (WGSR) should also contribute for the increase of CO_2 yield.

Fig. 6 presents the reusability of 0.5 wt% Cu-modified β-zeolite for bio-oil upgrading. The complete chemical identification of light oil in the upgraded bio-oil and the corresponding GC–MS spectra can be found in Table S2 and Fig. S4 of Supplementary data. One can see that the catalyst has good stability with less than 5% selectivity degradation when reused until three times. It should be noted that phenols, ether, and compounds with carboxyl functional group begin to appear in the light oil of upgraded bio-oil for the reused catalyst, which results in the increase of the oil yield. Fig. 7 depicts the mass balance of pyrolysis products as 0.5 wt% Cu-modified β-zeolite is reused without regeneration. By comparing Figs. 6 and 7, it can be seen that the appearance of carboxyl functional group is accompanied by the decrease of CO_2 yield, indicating the activity decrease for the decarboxylation reaction. However, it should be noted that the activity for the decarboxylation reaction can be maintained to some extent even though the reduction gas products (CO and H_2) decrease slightly. Herein, the slight decrease of CO and H_2O yields might be attributed to the accumulation of
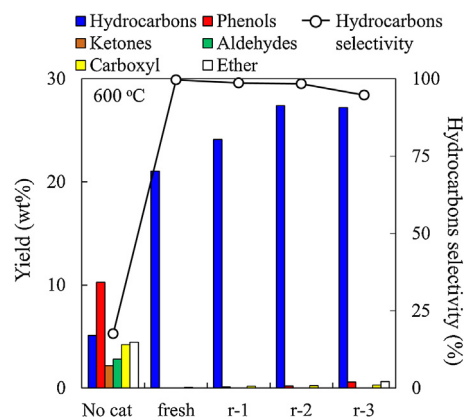

Fig. 6. Change of composition distributions in the light oil of upgraded bio-oils as 0.5 wt% Cu-modified β-zeolite is reused without regeneration.
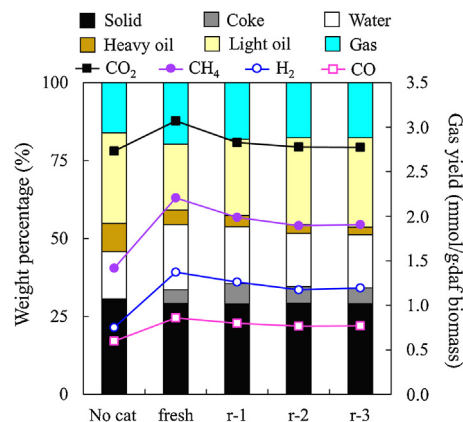

Fig. 7. Mass balance of the final products as 0.5 wt% Cu-modified β-zeolite is reused without regeneration.

Table 3
Total coke amount formed on the spent catalysts after four consecutive tests.

Cu loading (wt%)	Coke amount (mg/g spent catalyst)
0.00	102.3
0.25	71.0
0.50	71.9
1.00	74.7
3.00	78.5

coke which slightly degrades the deoxygenation activity. This result indicates that there is an optimum Cu loading amount for achieving the maximum catalytic performance with good reusability.

3.3. Analysis of coke deposit

Table 3 shows the total coke deposit amounts on the spent Cu-modified β-zeolites with different loading amounts after four consecutive reusability tests. Here, it should be noted that this quantification is different from that of coke estimation in mass balance of pyrolysis products which is carried out for each experiment and presented in percentage basis of initial biomass amount. One can see that less coke deposit is formed on the spent Cu-modified β-zeolites when comparing with the spent calcined β-zeolite. However, the total coke amount increases as the Cu loading amount increases due to the possibility of pore blockage. TPO profiles of spent catalysts shown in Fig. 8 reveal that the spent catalysts with 0.25 and 0.50 wt% of Cu loading amounts have the similar TPO peaks in intermediate and high temperature ranges as that of the spent calcined β-zeolite, implying that the carbon species
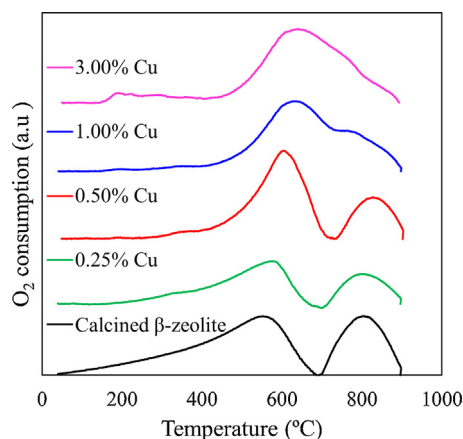
Fig. 8. TPO profiles of spent calcined β-zeolite and Cu-modified β-zeolites.

Table 4
Hydrocarbons classification in the presence and absence of catalysts.

Chemical compounds	No catalyst	Cu loading (wt%)				
		0.00	0.25	0.50	1.00	3.00
Aliphatic (wt%)	1.69	0.28	0.00	0.27	0.20	0.00
Benzene (wt%)	2.97	2.91	2.32	7.44	8.94	8.93
Toluene (wt%)	0.34	2.03	2.88	4.63	4.62	2.65
Xylene (wt%)	0.11	1.42	2.06	2.44	1.65	0.47
Other aromatic (wt%)	0.00	1.98	1.68	0.73	0.26	0.00
Polyaromatic hydrocarbon (wt%)	0.00	7.40	7.42	5.54	3.60	1.63

deposited on 0.25 and 0.50 wt% Cu-modified β-zeolites resembles to those on calcined β-zeolite. The slight difference on the peaks appeared at intermediate temperature is attributed to the small crystallinity difference of carbon species, which might be induced from the synergy effect of metal/metal-oxide sites and protonic sites in the Cu-modified β-zeolites with low Cu loading amount. In contrast, 1.00 wt% and 3.00 wt% Cu-modified β-zeolites show completely different TPO peaks, and the peak disappears at the high temperature range; especially some peaks appear in the lower temperature range for 3.00 wt% Cu-modified β-zeolite, indicating that some amorphous carbon species might also exist in the spent catalyst. It is widely known that the combustion temperature of carbon species relates to its degree of crystallinity [34,35]. Herein, considering the TPO profile of spent calcined β-zeolite as a reference, the TPO peaks at intermediate and high temperature ranges can be considered to correlate with the interaction of carbon deposit precursors (coke and/or soot) with protonic sites in the zeolite channels. Meanwhile, the TPO peaks at lower temperature correlate with the interaction of carbon deposit precursor with metal/metal-oxide sites on the outside surface of zeolite, which could result in the formation of amorphous carbon species. As such, for the high Cu loading amount, no carbon species can be detected at high temperature range, which confirms that the access of reactants, especially those large molecules entering into inner acid sites of zeolite structure should be considerably hindered due to the pore mouth blockage. By evaluating the peak shift at intermediate temperature, the carbon species at this temperature range might also correlates with Cu loading amount in the vicinity of zeolite support, which describes the synergy between metal/metal-oxide sites and protonic sites in the zeolite structure. One can consider that the contribution of metal/metal-oxide sites becomes more pronounced at higher Cu loading, which might change the deoxygenation route and reusability profile. These results also indicate that adjusting the Cu loading amount on β-zeolite could achieve the optimum catalytic performance with excellent reusability.

3.4. Mechanism of deoxygenation over Cu-modified β-zeolite

In our previous study [15], it is found that dehydration is more favorable over calcined protonic β-zeolite, which is proved by the increase of water content in the upgraded oil. In the present study, the water content is decreased as Cu loading amount is increased up to 1.00 wt%, but increased for higher Cu loading (3.00 wt%). It indicates that Cu loading favors the deoxygenation either from decarboxylation or decarbonylation with limited water formation. In the case of Cu loading amount, Cu species replace some of proton sites, resulting in a synergy effect between the metal sites

(isolated Cu species) and remaining proton sites (H⁺ cation). This synergy shifts the preferable route to decarbonylation with some contribution from dehydration reaction. Herein, the remaining proton sites could serve for the dehydration as well as decarboxylation of oxygenated compounds, meanwhile Cu sites promote the decarbonylation reaction [21]. CO and water generated from the dehydration reaction could experience water-gas shift reaction (WGSR) which further increases CO_2 and H_2, and decreases the water content. In other words, by replacing some of proton sites with metal sites, the occurrence of dehydration reaction should be decreased while that of decarbonylation reaction increased to some extent. This explains why the CO yield increases slightly while the water yield decreases.

As Cu loading amount is increased too high, some accesses to the inner proton sites and metal sites could be blocked so that the occurrence of decarbonylation over these metal sites decreases. As a result, ketones begin to appear and CO yield decreases slightly. Furthermore, in this case, the synergy between proton and metal sites also decreases considerably, resulting in the increase of phenols yield. For 0.5 wt% Cu-modified β-zeolite, it shows excellent reusability and almost no ketones and aldehyde are produced on it, indicating a good coking resistance, which should be attributed to this synergy effect. On the other hand, as has been explained above, CO_2 yield over 3.00 wt% Cu-modified β-zeolite increases due to the reduction of CuO cluster into metallic Cu. The metallic Cu gives the contribution on the dehydration reaction which results in the increase of water content.

In addition, β-zeolite modified by Cu also inhibits the formation of polyaromatic hydrocarbons. Table 4 presents the hydrocarbons classification of the obtained oil in the presence and absence of catalysts. When 0.25 wt% Cu is loaded on β-zeolite, benzene yield decreases at first while PAH yield increases. This could be due to the contribution of aromatization through Diels-Alder reaction, which can combine diene from cracked benzene with uncracked benzene to form naphthalene, resulting in the increase of naphthalene yield (Table S1) as well as overall PAH yield (Table 4). However, as Cu loading amount is increased, benzene yield increases while naphthalene and the total PAH yields decreases to some extent. These results are in contrary with the previous reports [36,37], where the supported Cu catalysts show good activity for the Diels-Alder reaction. In this study, the deoxygenation over Cu-modified β-zeolite is realized through dehydration, decarboxylation and decarbonylation, and the synergy effect between proton sites and metal sites seem to dominate the process. Furthermore, one can see that the change of Cu loading amount can alter the proportion of hydrocarbon contents, including aromatic and PAH compounds. It is expected to obtain the different target products using this way.

4. Conclusions

Catalytic upgrading of bio-oil over Cu-modified β-zeolite catalysts with various Cu loading amounts in a down-draft fixed-bed reactor is performed, and the following results are obtained:

(1) Calcined β-zeolite itself has high selectivity to the hydrocarbon in the bio-oil upgrading. However, coking is also easily formed on it.

(2) When high silica β-zeolite is modified by a small amount of Cu, the selectivity to the hydrocarbons can be obviously promoted, and less carbon species will be formed on them. Especially, when 0.50 wt% of Cu is loaded on it, almost only hydrocarbons can be detected in the light oil of upgraded bio-oil. However, if more Cu is loaded, the selectivity decreases to some extent.

(3) The activity of 0.50 wt% Cu-modified β-zeolite can be remained for several reuses even without regeneration treatment.

(4) Loading of Cu on β-zeolite results in the increase of surface area as well as the formation of more micropores. Especially, the surface area reaches the maximum in the case of 0.50 wt% of Cu doping. It is found that Cu species aggregate on the surface of zeolite when the loading amount is over 1.00 wt%, which results in the blockage of zeolite pores as well as the decrease of surface area.

(5) These results indicate that the synergetic effect between the doped metal sites and the proton sites on the zeolite structure should be benefit for the promising catalytic performance and thus, a proper loading amount is very important for this kind of catalyst.

Acknowledgements

Appendix A. Supplementary data

Supplementary data associated with this article can be found, in the online version, at http://dx.doi.org/10.1016/j.apcatb.2016.01.006.

References

[1] Y. Fan, Y. Cai, X. Li, H. Yin, N. Yu, R. Zhang, W. Zhao, J. Anal. Appl. Pyrol. 106 (2014) 63–70.
[2] F. Abnisa, A. Arami-Niya, W.M.A. Wan Daud, J.N. Sahu, I.M. Noor, Energy Convers. Manage. 76 (2013) 1073–1082.
[3] S. Xiu, A. Shahbazi, Renew. Sustain. Energy Rev. 16 (2012) 4406–4414.
[4] T.S. Nguyen, M. Zabeti, L. Lefferts, G. Brem, K. Seshan, Bioresour. Technol. 142 (2013) 353–360.
[5] P.K. Kanaujia, Y.K. Sharma, M.O. Garg, D. Tripathi, R. Singh, J. Anal. Appl. Pyrol. 105 (2014) 55–74.
[6] K. Jacobson, K.C. Maheria, A. Kumar Dalai, Renew. Sustain. Energy Rev. 23 (2013) 91–106.
[7] A. Demirbas, Appl. Energy 88 (2011) 17–28.
[8] X. Li, R. Gunawan, Y. Wang, W. Chaiwat, X. Hu, M. Gholizadeh, D. Mourant, J. Bromly, C.-Z. Li, Fuel 116 (2014) 642–649.
[9] J. Lehto, A. Oasmaa, Y. Solantausta, M. Kytö, D. Chiaramonti, Appl. Energy 116 (2014) 178–190.
[10] Y. Zhang, T.R. Brown, G. Hu, R.C. Brown, Chem. Eng. J. 225 (2013) 895–904.
[11] R. Nava, B. Pawelec, P. Castaño, M.C. Álvarez-Galván, C.V. Loricera, J.L.G. Fierro, Appl. Catal. B 92 (2009) 154–167.
[12] F. Li, Y. Yuan, Z. Huang, B. Chen, F. Wang, Appl. Catal. B 165 (2015) 547–554.
[13] B. Valle, A.G. Gayubo, A. Alonso, A.T. Aguayo, J. Bilbao, Appl. Catal. B 100 (2010) 318–327.
[14] H.J. Park, H.S. Heo, J.-K. Jeon, J. Kim, R. Ryoo, K.-E. Jeong, Y.-K. Park, Appl. Catal. B 95 (2010) 365–373.
[15] W.B. Widayatno, G. Guan, J. Rizkiana, X. Du, X. Hao, Z. Zhang, A. Abudula, Bioresour. Technol. 179 (2015) 518–523.
[16] K. Tarach, K. Góra-Marek, J. Tekla, K. Brylewska, J. Datka, K. Mlekodaj, W. Makowski, M.C. Igualada López, J. Martínez Triguero, F. Rey, J. Catal. 312 (2014) 46–57.
[17] K.K. Ramasamy, M.A. Gerber, M. Flake, H. Zhang, Y. Wang, Green Chem. 16 (2014) 748–760.
[18] H.W. Lee, S.J. Choi, S.H. Park, J.-K. Jeon, S.-C. Jung, S.H. Joo, Y.-K. Park, Energy 66 (2014) 2–6.
[19] S. Vitolo, M. Seggiani, P. Frediani, G. Ambrosini, L. Politi, Fuel 78 (1999) 1147–1159.
[20] P.T. Williams, P.A. Horne, J. Anal. Appl. Pyrol. 31 (1995) 39–61.
[21] A. Veses, B. Puértolas, M.S. Callén, T. García, Microporous Mesoporous Mater. 209 (2015) 189–196.
[22] R. Cid, Catal. Lett. 24 (1994) 147–157.
[23] E.F. Iliopoulou, S.D. Stefanidis, K.G. Kalogiannis, A. Delimitis, A.A. Lappas, K.S. Triantafyllidis, Appl. Catal. B 127 (2012) 281–290.
[24] Z. Du, X. Ma, Y. Li, P. Chen, Y. Liu, X. Lin, H. Lei, R. Ruan, Bioresour. Technol. 139 (2013) 397–401.
[25] R. French, S. Czernik, Fuel Process. Technol. 91 (2010) 25–32.
[26] Y.T. Cheng, J. Jae, J. Shi, W. Fan, G.W. Huber, Angew. Chem. Int. Ed. 51 (2012) 1387–1390.
[27] M. Guisnet, P. Magnoux, Catal. Today 36 (1997) 477–483.
[28] S. Vitolo, B. Bresci, M. Seggiani, M.G. Gallo, Fuel 80 (2001) 17–26.
[29] W.B. Widayatno, G. Guan, J. Rizkiana, X. Hao, Z. Wang, C. Samart, A. Abudula, Fuel 132 (2014) 204–210.
[30] S.E. Wanke, P.C. Flynn, Catal. Rev. Sci. Eng. 12 (1975) 93–135.
[31] B. Pereda-Ayo, U. De La Torre, M.J. Illán-Gómez, A. Bueno-López, J.R. González-Velasco, Appl. Catal. B 147 (2014) 420–428.
[32] F.A. Diaz-Mendoza, L. Pernett-Bolano, N. Cardona-Martinez, Thermochim. Acta 312 (1998) 47–61.
[33] P. Forzatti, L. Lietti, Catal. Today 52 (1999) 165–181.
[34] A.H. Fakeeha, W.U. Khan, A.S. Al-Fatesh, A.E. Abasaeed, Chin. J. Catal. 34 (2013) 764–768.
[35] I.H. Son, S.J. Lee, I.Y. Song, W.S. Jeon, I. Jung, D.J. Yun, D.-W. Jeong, J.-O. Shim, W.-J. Jang, H.-S. Roh, Fuel 136 (2014) 194–200.
[36] S. Reymond, J. Cossy, Chem. Rev. 108 (2008) 5359–5406.
[37] N.A. Caplan, F.E. Hancock, Catalysts, Google Patents, 2007.